Optimal Design of Magnetic Springs; Enabling High Life Cycle Elastic Actuators

Branimir Mrak [a,b], Bert Lenaerts[b], Walter Driesen [b], Wim Desmet [a]

[a] Department of Mechanical Engineering, Katholieke Universiteit Leuven, Celestijnenlaan 300 B, B-3001 Leuven, Belgium
[b] Flanders Make vzw, Celestijnenlaan 300 C, B-3001 Leuven, Belgium,

***Abstract*—Magnetic springs are an energy storage alternative to mechanical springs in applications that require long lifetime with no fatigue failure. Although this concept exists in academia for more than 30 years, industrial applications have been sparse. The goal of this article is twofold: (i) to position magnetic springs side-to-side with mechanical springs and (ii) develop a design methodology that will allow us to improve dynamic performance and/or reduce average and peak power consumption in highly dynamic industrial motion systems. Additionally, an extensive exploration of industrially feasible magnetic spring design space is performed using 2D finite element models combined with multi-objective genetic algorithm, resulting in Pareto-optimal fronts and parameter sets for each of the studied topology. Aside from geometry optimization, different magnetizations and permanent magnet materials are studied. Modelling efforts are validated on a physical prototype using both static and dynamic measurements of a two-pole magnetic spring within a dedicated setup. The validated results will be used within this paper to position magnetic spring assisted actuators back-to-back with classical industrial solutions.**

I. Elastic Actuators and Magnetic Springs - Outlook

The principles of elastic actuation, first introduced by Alexander et al.[1], whether series [2] or parallel [3] elastic actuators, have been consistently proven to improve actuator performance in service robotics. These systems rely on high torque and force density of mechanical springs to reduce peak power requirements and improve actuator's energy efficiency. For example, in work done by Mettin et al. [4] the energy consumption is reduced by 55%.

A mechanical spring stores energy as the potential energy of elastic deformation. Spring design for highly dynamic loads in industrial use is typically limited by the long lifetime requirements and often leads to suboptimal designs for purposes of elastic actuation. Traditionally, it was considered that for some metals there is a stress level called fatigue limit, that can be sustained with an infinite lifetime [5]. Nowadays, this value is still often used in design together with the stochastic design methods. However, the existence of fatigue limit has been disputed even in the lab environment due to inclusions in the crystal lattice [6] of steels. Local stresses can lead to fatigue in any kind of metallic springs [5][8] and industrial environments impose additional risks (i.e. corrosive environment, temperature variations, mechanical handling, manufacturing limitations etc.). Often, high safety factors are employed to guarantee a robust design for a full product line.

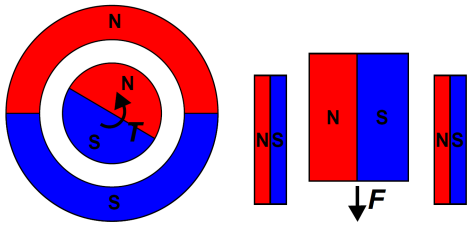

Figure 1. Conceptual drawings of a torsional and translational magnetic springs

Although the functionality of the magnetic spring (fig. 1) can be compared to that of a mechanical spring, the underlying physical principles are utterly different. Magnetic springs store potential energy in the magnetic field of permanent magnets, where no fatigue failure mechanism is involved and thus have a virtually infinite lifetime [14], assuming the device is properly designed. This allows the use of compliant actuation concepts [11] in highly dynamic industrial applications with stringent lifetime demands.

With elastic actuators, it is possible to deliver more mechanical reactive power to the system under the assumption of higher torque density of springs compared to motors. Considering the evident benefit of using mechanical springs in service robotics in improving dynamic behavior, it is necessary to prove that magnetic springs have the same or higher energy density than conventional solutions with mechanical springs, in order to showcase their potential for the design of industrial motion systems. Some of the target applications are torque oscillation compensation in continuous rotation in internal combustion engines and windmills, reciprocating and intermittent motion in weaving looms [9], fast switching valves [13] (valvetrains in internal combustion engines), reciprocating pumps and compressors [10] and other tools and machines with highly dynamic reciprocating motion. Additionally, magnetic springs have been reported for use in vibration reduction and vibration isolation [15] as well as for static load compensation [16].

It is worth mentioning that magnetic springs are topologically identical to passive magnetic bearings(PMB) and magnetic clutches. The main difference is the magnetic load point of the permanent magnets: in a magnetic spring the magnets are loaded over the entire B-H curve in each loading cycle, while for PMB and clutches the operating point remains constant for a constant mechanical load.

Unlike the previous efforts on the topic [9][10][11][13][14]], where the effort was focused on a specific use case, this paper

studies optimal design of magnetic spring in more detail and demonstrates systematically the impact of magnetic spring on the performance of highly dynamic industrial actuators.
The work is organized as follows: in section II, the developed design methodology for magnetic springs is presented, with both the detailed component design approach and the link with a scalable 1D model to be used for system design; In section III validation of the modelling approach is presented for a selected optimal design; Section IV presents the detailed component optimization results and offers insight into magnetic spring design, as well as impact of the component design on the system performance.

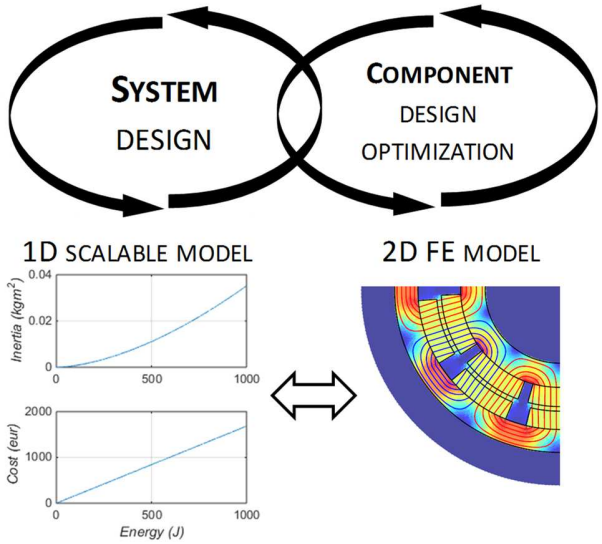

Figure 2. Codependent nature of system design cycle and component design cycles through linked modelling approaches

II. Design Methodology

Within this article, the focus is primarily on component design cycle, but we will also present its complementarity with the system design cycle (fig. 2).
Although FE model of a detailed design geometry is an indispensable tool for component design, in system optimization the computational cost of FE can be prohibitively expensive. On the other hand, a scalable 1D dynamic model of a magnetic spring is the ideal model for sizing of different drivetrain components and system optimization.
Therefore, we define a 1D scalable model based on first principles, where cost and inertia of a magnetic spring are calculated directly from required reactive energy. This model can be iteratively updated based on the FE model results, as a result of the virtual validation where 1D model is compared to optimal component designs coming from component optimization design.

A. Scalable 1D models based on first principles

A standard way to compare energy-storing devices is a Ragone chart [17]. It typically shows the tradeoff between energy density and power density, i.e. some energy storage components should be used when high energy density is required (e.g. Li-ion batteries) and others when high instantaneous power is required (supercapacitors, flywheels). The bottleneck of such a static approach when it comes to highly dynamic drivetrains is the disregard for lifetime and system dynamics. In the highly dynamic applications targeted within this study, the mechanical power delivered to the system is significantly limited by the actuator bandwidth.
Therefore, it is necessary to know the inertia of the spring alongside with the torque characteristic. Phenomenologically we can analyze the spring density of a spring. For elastic springs this will be the surface under the stress-strain curve (for the linear elastic model where the relation of stress and strain is linearly described by Young's modulus). Equivalently, for an idealized magnetic spring energy density is equivalent to the surface under the BH curve (fig. 3), which is approximately 2 times the $BHmax$ product.

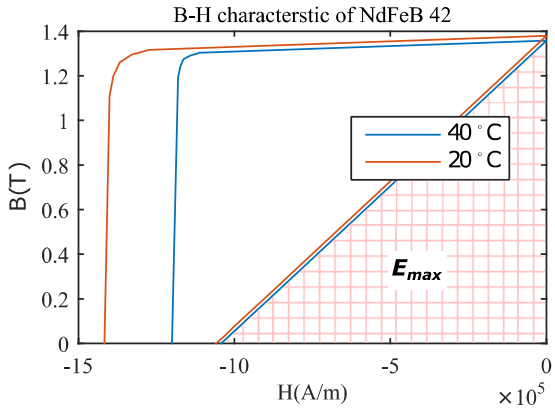

Figure 3. Potential energy of permanent magnet calculated from B-H characteristic is a measure of maximum theoretical energy density of a magnetic spring

Two assumptions about the magnetic spring have to be made in order to create a 1D scalable model. First of all, equal distribution of magnets between stator and rotor, resulting in perfect canceling of the magnetic field in the magnets in the case where maximum potential energy is stored within the magnet. Secondly, a fixed form factor of the rotor – following the 1st assumption and optimal rotor diameter achieved from FE simulation.

TABLE I. Overview of Considered Permanent Magnet Materials

Grade	***33H***	***42H***	***Pi-95HR***
Energy density $[kJ = m^3]$	521	673	173
$BHmax$ $[kJ = m^3]$	263	334	85
Max temperature $[°C]$	120	120	125
Available magnetizations	Limit*	Limit*	Free**

(*) Sintered NdFeB - anistropic material
(**) Plasto- bonded NdFeB - isotropic material

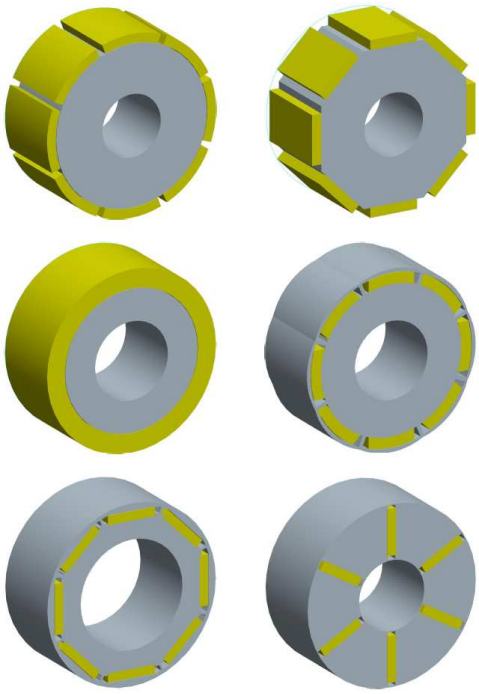

Figure 4. Overview of parametrized PM rotor topologies used in design optimization with surface mounted topologies a-c being most suitable for high torque density

Furthermore, realistic designs of a magnetic spring will always have a lower energy density than the maximum theoretical limit, due to flux leakage. Therefore, we can define the design efficiency as a ratio of energy densities of a realistic magnetic spring and an ideal magnetic spring

$$\eta_{mat} = \frac{E_{FE}}{E_{max}} \qquad (1)$$

and use it for 1D model correction based on FE results.

B. Detailed component design of magnetic springs

For the realistic embodiment of the magnetic spring concept, there is a range of feasible variants, both continuous (geometry sizing) and discrete (topological, material selection). By permutation of the discrete variants (Table I), we can generate a number of topologies, of which a number can be pruned out early in the design. The remaining, promising topologies were optimized and studied in more detail using MagOpt software [12].

TABLE II. OVERVIEW OF EVALUATED TOPOLOGIES

Property	Variant
PM material	Isotropic, anisotropic, temperature grade
Magnetization	Straight/ diametrical, radial/ tangential, Halbach
Magnetic array	Quasi-Halbach, multipole, over-segmented pole
Magnet shape	Arc segment, rectangular, bread loaf
Magnet mounting	Surface, buried, internal

When setting up the design specifications, it important to note that magnetic spring will not necessarily have a linear characteristic. Except in the case of using them with small strokes around equilibrium positions, it is more likely to produce a quasi-sinusoidal characteristic. The above mentioned quasi-linear region can be extended by specific geometries of the magnet and back-iron. However, this can lead to lower design efficiency. Additionally, it is not a given fact that a linear characteristic is the most suitable solution for a given application case. An example of utilizing nonlinear spring can be found in [18] where stable and unstable equilibria of magnetic spring can be used instead of a locking mechanism. Under this consideration, we need an alternative to spring stiffness to translate the system design specifications into component design specifications.

Specifying stroke and potential energy of a spring is adequate since it does not over-constrain the optimization problem by imposing a desired torque characteristic. The magnetic spring potential energy can be evaluated from torque characteristic and stroke as

$$E = \int_{\theta_1}^{\theta_2} T(\theta) d\theta \qquad (2)$$

In order to evaluate each design variant, a 2D magnetostatics model of the geometry is calculated (Fig. 5).

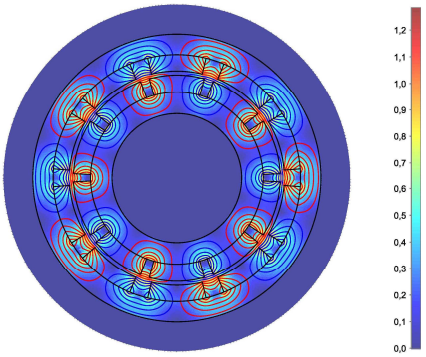

a) Anti- alligned magnets resulting in unstable equlibrium with maximum energy stored in PM

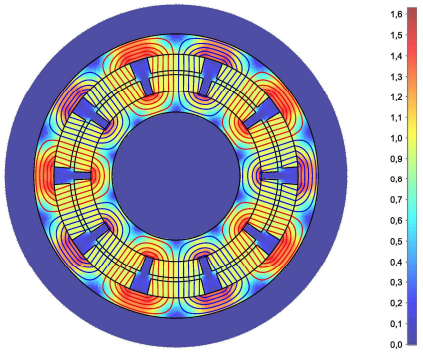

b) Alligned magnets resulting in stable equilibrium - 0 energy stored in PM

Figure 5. Single design evaluation of a 5 pole magnetic spring with surface mounted arc magnets; Flux lines ploted over B(T)

For long rotors with the aspect ratio of length to diameter of more than 2, the 2D approach should be sufficient. For disc geometries, it would be necessary to use a 3D model. Since we are interested in high bandwidth actuators, it makes sense to focus on low inertia, long shaft solutions.

For each finite element model evaluation, a list of metrics of interest can be calculated, either by pre-processing the specifications and the geometry or post-processing the FE solution. The considered design metrics are:

1) Torque characteristic
  a) Stored energy
  b) Stroke
  c) Higher harmonic content (Fourier/ THD)
2) Inertia
3) Bulk material cost
4) Demagnetization

The main objective of the design is to make a spring that fits the described energy and stroke specifications while minimizing inertia and cost.

For a thorough design optimization, package MagOpt was used [12] together with an opensource 2D FE solver for magnetostatic problems [19]. Other listed metrics were monitored for reasons of design safety (demagnetization) and possible unwanted dynamic effects (higher harmonic content). So far loss models have not been considered, assuming that the efficiency of a magnetic spring to be very high compared to a servo-drive since ohmic losses and the drive losses are completely avoided [20].

III. Prototyping and Experimental Validation

A. Prototype and component validation

In order to validate the modeling approach described in section III-C, a prototype of a magnetic spring has been built using NdFeB N42H ring magnets (fig. 6).

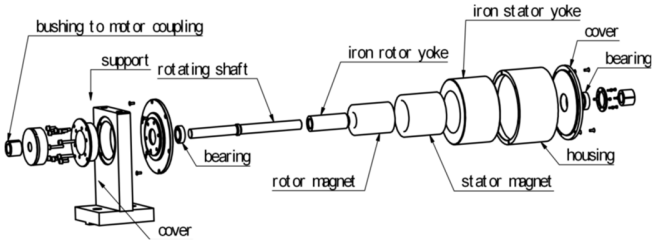

Figure 6. Explosion view of the prototyped magnetic spring design

A test rig (fig. 7) composed of the magnetic spring prototype, highly dynamic PMSM, two dynamic torque sensors and a tunable inertia flywheel was used to obtain a static measurement (fig. 8) to validate 2D FEM. Additionally, a dynamic motion experiment was conducted in order to validate the hypotheses of low losses in the magnetic spring compared to the PMSM with a similar torque profile.

The results of measurement show a good qualitative and quantitative fit of static measurement and a good qualitative fit with respect to low loss hypothesis. In fig. 9, a slight skewing (max. 15 degrees) of sinusoidal curve is visible. This phenomenon is expected to be related to the eccentricity of the

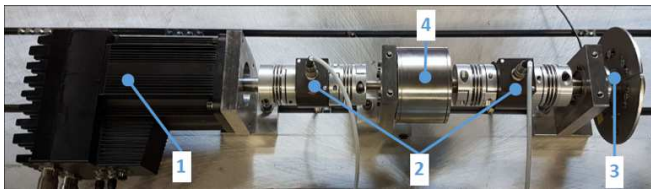

Figure 7. Test rig consisting of a (1) servo-drive, (2) torque sensors, (3) flywheel – load and the developed prototype of a magnetic spring (4)

magnetic center of design and the mechanical rotation axis due to the manufacturing tolerances. Nevertheless, the peak torque value has less than 1% error compared to the FE model.

As a dynamic measurement, power flow from and into a spring was measured using the above-mentioned torque and position sensors. A roundtrip efficiency of 94% has been calculated for a full trajectory at a frequency of 5Hz, based on dynamic measurements from torque sensor and encoders, where roundtrip efficiency can be defined as

$$\eta_{RT} = \frac{E_{out}}{E_{in}} = \int \Delta T_{meas} \omega dt \quad (3)$$

where ΔT_{meas} is the dynamic differential torque measurement obtained from the two torque sensors and ω is the rotational velocity of the rigid shaft.

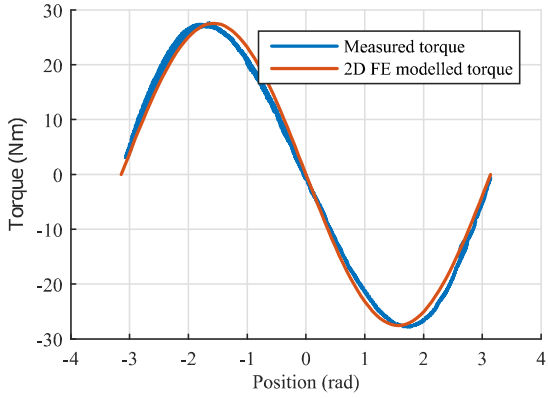

Figure 8. Static measurement of magnetic spring torque characteristic

B. System performance – reciprocating drivetrain

The magnetic spring assisted drivetrain shown in fig. 5 can be operated between the unstable equilibria, similar to a parallel elastic actuator with a locking mechanism [4] or an inverted pendulum.

The system is operating as follows (fig. 9). At *t=-0s* load is held in a stable equilibrium. Initially a a FF pulse torque pulse is applied together with a negative damping controller in order to excite the natural resonance of the system (phase 1. Start-up). Due to the negative damping the load is slowly brought in the neighborhood of the unstable equilibrium where a stable PID controller is switched on in order to hold the load in position with 0-torque control (phase 2. 0- torque wait). Once a reciprocating motion is required the controller is operating in a catch-release fashion with a small FF torque pulse initiating the motion and pushing the load towards the next unstable equilibrium. Due to the magnetic spring torque, the load is

accelerated until reaching the middle point, where the spring starts to decelerate the load. Upon reaching the surroundings of the next unstable equilibrium, the motor is activated again, with a feedback controller, in order to stabilize the load in the endpoint. In this fashion, the motor is delivering only the bare minimum of the required torque.

The same motor operating without a magnetic spring while driving the same load (fig.9), requires a peak torque of 25Nm while in case of the magnetic spring assisted setup it is only 8Nm. Therefore, the required peak torque is approximately 3 times lower in case where a magnetic spring is used.

The significant reduction can also be observed in energy consumption per cycle of reciprocating motion. Energy required for operation of magnetic spring assisted drivetrain is reduced from 29.07J per cycle to 5.05J per cycle, signifying an almost 6 fold energy reduction. Energy consumption is calculated as a sum of the measured mechanical power (torque sensors, encoders) at the motor output shaft and the ohmic losses calculated from the torque reference and phase

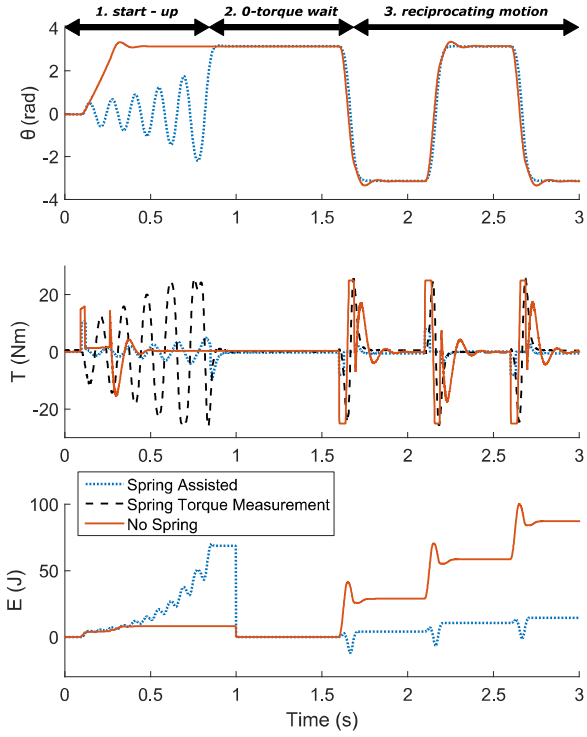

Figure 9. Experimental validation – comparison of dynamic operational data for a magnetic spring with minimum motor torque vs. no spring setup with peak torque operation

It is visible that initially, during the start-up the energy required to initialize the spring assisted setup is higher. This is, however, not a serious downside of the spring assisted actuator considering that in the industrial application cases the drivetrain is only seldomly initiated before long hours of operation, making the start-up energy consumption a negligible segment of the total energy consumption. For this reason, and for convenience of tracking the energy consumption during the operational behavior (phase 3. Reciprocating motion) the plotted energy is reset during the 0 torque wait.

Alternatively, it is also possible to run the spring assisted system at a much higher torque in order to achieve a faster transient than it is possible with the motor only. In that case, a bang-bang controller can be used to accelerate the load as quickly as possible between two end positions.

IV. Optimization Results and Impact on System Performance

Detailed design optimization of the selected 5 most interesting topologies was done. As a result, it is possible to compare Pareto fronts for different magnetic spring topologies for a fixed energy requirement and stroke. On fig. 10 it can be seen that sintered NdFeB is preferred over bonded magnets for reasons of both lower cost inertia.

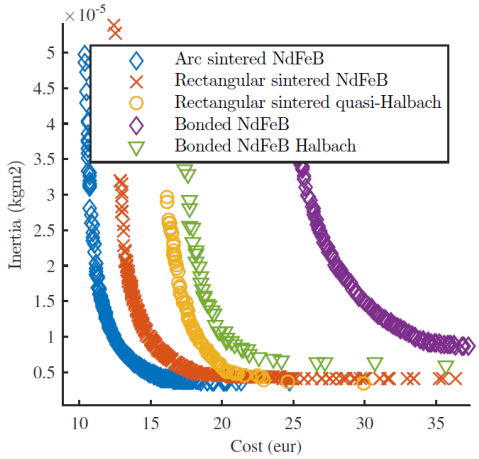

Figure 10. Optimization results plotted as Paret-fronts for 5 selected stator and rotor topologies selected after design space pruning

The added value of using isotropic material (bonded NdFeB) to achieve a wider variety of magnetization is smaller than the added cost and inertia that results from lower flux densities in these materials. Interestingly, low inertia levels can be achieved for each topology, irrelevant of the magnet geometry. However, the amount of material required to do so results in the lowest cost design with surface mounted arc magnets.

Additional conclusions regarding design rules can be drawn from optimization results through Pareto optimal parameters. In fig. 11 normalized histograms (non- dimensional value on y axis) of the pareto optimal designs are plotted for each of the 5 selected topologies, showing the parameter distribution for the optimal designs that lie on the Pareto front.

It is noticeable that that stator and rotor parameter distribution demonstrate a symmetry (left and right side of fig. 11), validating the idea of evenly distributed magnets between stator and rotor resulting in optimal magnetic spring design.

Further analysis, shows that pole pitch in quasi Halbach arrays is optimally fully pitched with pitch factor values (i.e. the ratio of magnet coverage and pole pitch) approaching 1 (fig. 11e and fig. 11f), which results in closest possible design to a real Halbach magnetization. On the other hand, standard multipole array values optimally have short pitch poles with pitch factor values between 0.75 and 0.85 in order to prevent short-

circuiting of the permanent magnet flux. The specific value of pitch factor, in this case, depends on the magnetic air gap between stator and rotor magnets as this represents the magnetic resistance of the parallel flux path. Another difference between Halbach and standard multipole arrays is in the thickness of the magnets (fig. 11c and fig. 11d).

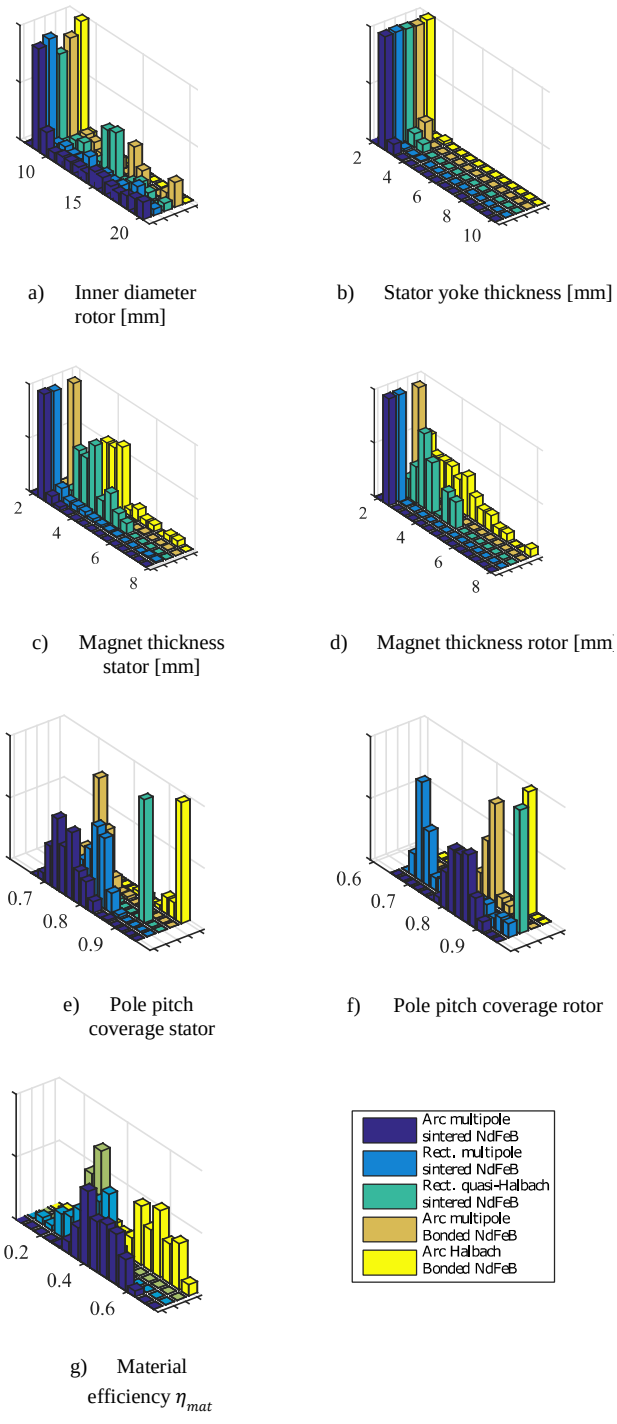

a) Inner diameter rotor [mm]

b) Stator yoke thickness [mm]

c) Magnet thickness stator [mm]

d) Magnet thickness rotor [mm

e) Pole pitch coverage stator

f) Pole pitch coverage rotor

g) Material efficiency η_{mat}

Figure 11. Optimal parameters histograms for 5 selected stator and rotor topologies selected after design space pruning

Following the optimization results, the impact of magnetic spring on system performance can be analyzed from different perspectives.

To compare magnetic springs to mechanical springs side-to-side phenomenologically, maximum theoretical energy density based on first principles is considered alongside with the realistically feasible energy density following from the optimization result. Since desired lifetime has a direct influence on stress level in mechanical springs and therefore also on energy density, we can plot energy density vs. required lifetime for mechanical and magnetic springs (fig. 12).

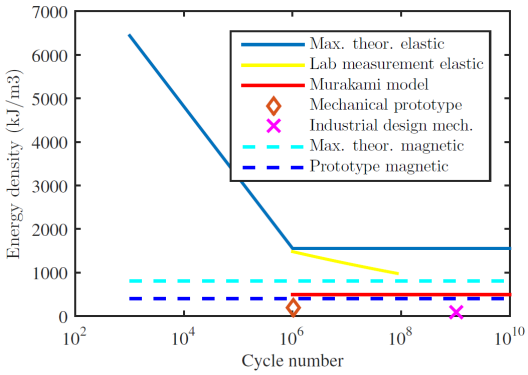

Figure 12. Magnetic springs vs. mechanical springs – magnetic springs have increasingly higher energy denisty for high life cycle numbers from 10^7 and beyond

Maximum theoretical energy density of magnetic spring of $E_{max52S} = 828kJ/m^3$ is already higher than that of the Murakami model based gigacycle energy density of steel springs at $E_{Murakami} = 506kJ/m^3$. The difference between feasible energy density achieved with the feasible designs is even more dramatic. With NdFeB 42H grade and arc magnets we are able to design a magnetic spring with energy density of $E_{model42H} = 404kJ/m^3$, while a specific mechanical springs described in [9] possesses an energy density of $E_{mech} = 210kJ/m^3$ with possible fatigue failure already at megacycles However, it is difficult to generalize on feasible gigacycle mechanical designs for all the designs as the range of safety factors used within these applications is usually in quite a large range. Nevertheless, while being conservative we can say that the resulting increase in energy density is at least 50%.

Relying on the simplistic scalable models of PMSM [21] and the scalable 1D model from this article we can analyze the performance of a magnetic spring alongside PMSM. The available peak torque T_{peak} of a synchronous motor and a magnetic spring are plotted versus their moment of inertia J. Several types of servomotors are considered, among which the most dynamic that could be found on the market. Extrapolation from the datasheet points is carried out using the relation

$$J = {T_{peak}}^{5/3} \qquad (3)$$

which is valid for both springs and motors, assuming a fixed rotor aspect ratio (diameter/length). To reduce cost and size of an electric drive solution, a reducer with transmission ratio n

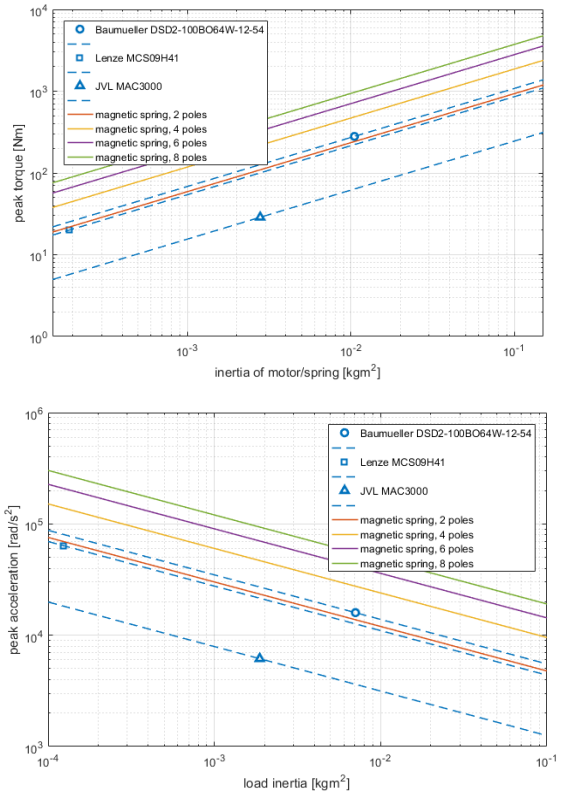

Figure 13. Magnetic springs torque density and achievable benchmarked against off the shelf PMSM solutions for highly dynamic loads

may be employed. However, the reflected inertia with a geared solution is always higher, given that $J = n^2 J_{motor}$ and $2 > 5/3$.

Also plotted is the maximum acceleration that can be achieved on a given inertial load. The peak acceleration follows from the available peak torque and the motor/spring inertia. For the relation given above, it can be derived that maximum acceleration occurs when $J = \frac{3}{2} J_{load}$.

It must be noted that only peak torques are considered here, which are limited by the magnetic design of motor and spring. For motors, the allowable nominal torque depends on the thermal design. Magnetic springs have no such limitation, since there are no losses associated with torque generation.

It can be concluded that, as a result of high torque density of magnetic springs the actuator bandwidth can be systematically improved for predetermined reciprocating profiles. For exact validation of this results and the value obtained in section III.B terms of energy and bandwidth, a more detailed study on system optimization of magnetic spring assisted drivetrains will follow as future work.

V. Conclusion

A method for component design of rotational magnetic spring is developed and validated. A theoretical energy density was established based on physical insight in energy stored in permanent magnets. Detailed design optimization results show that design up to 60% of material efficiency are manufacturable. Best results are achieved with surface mounted arc sintered NdFeB magnets.

The modelling approach is validated by component characterization on the experimental test rig. The impact of magnetic spring on system behavior are experimentally demonstrated with six times lower energy consumption, and three times lower peak torque for a magnetic spring assisted drivetrain.

Following these results, based on 1D scalable models of magnetic springs, energy density of mechanical and magnetic spring can be compared for long lifetime. Magnetic springs have at least a 50% higher power/energy density than mechanical springs with the with the added benefit of no fatigue failure.

Additionally, using 1D scalable models of magnetic springs, a comparison between torque density of magnetic springs and PMSM off-the-shelf motors shows the added value of magnetic springs for preplanned reciprocating motion systems. The added benefit is specifically dramatic for partial strokes when magnetic springs with two and more pole pairs are employed, when drivetrain peak acceleration is increased by at least 33%.

Future detailed studies into system level design of reciprocating systems are expected to quantify the associated cost reduction resulting from possible motor downsizing and improvement in energy efficiency.

Moreover, it is important to notice that for magnetic spring design demagnetization is still a possible issue. Demagnetization H_{demag} field is directly influenced by the temperature, and the rise in temperature is directly caused by losses. Although, based on the dynamic measurement performed on the prototype, magnetic spring losses do not seem to be relevant for the design of spring assisted reciprocating drivetrains, a better understanding of thermal behavior and losses might lead to savings related to the selection of lower temperature grade magnets related to lower Dysprosium content.

Acknowledgement

The authors would like to thank Linz Center of Mechatronics GmbH and dr. Siegfried Silber for their support through usage of MagOpt software and the associated infrastructure.

The research of B. Mrak as an Early Stage Researcher is funded by a grant within the European Project EMVeM Marie Curie Initial Training Network (GA 315967).

This research was partially supported by Flanders Make, the strategic research centre for the manufacturing industry within Flanders Make project Profensto_icon.

References

[1] R. M. Alexander, “Three Uses for Springs in Legged Locomotion,” The International Journal of Robotics Research, vol. 9, no. 2, pp. 53–61, 1990.

[2] D. Paluska and H. Herr, “The effect of series elasticity on actuator power and work output: Implications for robotic and prosthetic joint design” *Robotics and Autonomous Systems, vol. 54, no. 8, pp. 667–673, 2006.*

[3] B. Vanderborght, B. Verrelst, R. Van Ham, M. Van Damme, D. Lefeber, Y. Duran and P. Beyl, “Exploiting natural dynamics to reduce energy consumption by controlling the compliance of soft actuators,” *The*

International Journal of Robotics Research, vol. 25, no. 4, pp. 343–358, 2006.

[4] U. Mettin, P. X. La Hera, L. B. Freidovich, and a. S. Shiriaev, “Parallel Elastic Actuators as a Control Tool for Preplanned Trajectories of Underactuated Mechanical Systems,” The International Journal of Robotics Research, vol. 29, no. 9, pp. 1186–1198, 2010.

[5] C. Bathias and P. C. Paris, Gigacycle fatigue in mechanical practice, 2005.

[6] R. Puff and R. Barbieri, “Effect of non-metallic inclusions on the fatigue strength of helical spring wire,” Engineering Failure Analysis, vol. 44, pp. 441–454, 2014.

[7] T. Abe, Y. Furuya, and S. Matsuoka, “Gigacycle fatigue properties of 1800 MPa class spring steels,” Fatigue & Fracture of Engineering Materials & Structures, vol. 27, no. 2, pp. 159–167, 2004.

[8] E. M. Serbino and A. P. Tschiptschin, “Fatigue behavior of bainitic and martensitic super clean Cr Si high strength steels,” International Journal of Fatigue, vol. 61, pp. 87–92, 2014.

[9] B. Mrak, W. Driesen, and W.Desmet, “Magnetic springs - Fast Energy Storage for Reciprocating Industrial Drivetrains,” In Conference Proeedings of 23rd ABCM International Congress of Mechanical Engineering, vol.COB-2015-2727, Rio de Janeiro, Brazil

[10] F. Poltschak, “A high efficient linear motor for compressor applications,” Power Electronics, Electrical Drives, Automation and Motion (SPEEDAM), 2014 International Symposium on, 2014, pp. 1356 – 1361., 2014.

[11] A. Sudano, N. L. Tagliamonte, D. Accoto, and E. Guglielmelli, “A resonant parallel elastic actuator for biorobotic applications,” in IEEE International Conference on Intelligent Robots and Systems, September, 2014, pp. 2815–2820.

[12] S. Silber, W. Koppelstatter, G. Weidenholzer, and G. Bramerdorfer, “MagOpt - Optimization Tool for Mechatronic Components,” 14th International Symposium on Magnetic Bearings, vol. 4, pp. 243–246, 2014.

[13] B. A. Reinholz, R. J. Seethaler, and A. Electromechanical, “Experimental Validation of a Cogging-Torque-Assisted Valve Actuation System for Internal Combustion Engines,” vol. 21, no. 1, pp. 453–459, 2016.

[14] P. J. Patt, “Design and Testing of a Coaxial Linear Magnetic Spring with Integral Linear Motor,” IEEE Transactions on Magnetics, vol. MAG-21, no. 5, pp. 1759–1761, 1985.

[15] T. Mizuno, M. Takasaki, D. Kishita, and K. Hirakawa, “Vibration isolation system combining zero-power magnetic suspension with springs,”Control Engineering Practice, vol. 15, no. 2, pp. 187–196, 2007.

[16] J. Boisclair, P.-l. Richard, and T. Lalibert, “Gravity Compensation of Robotic Manipulators Using Cylindrical Halbach Arrays,” vol. 22, no. 1, pp. 457–464, 2017.

[17] T. Christen and C. Ohler, “Optimizing energy storage devices using Ragone plots,” Journal of Power Sources, vol. 110, no. 1, pp. 107–116, 2002.

[18] C. King, J. J. Beaman, S. V. Sreenivasan, and M. Campbell, “Multistable equilibrium system design methodology anddemonstration,” Journal of Mechanical Design, vol.126, no. 6, pp. 1036–1046, 2005.

[19] D. Meeker, “FEMM.”

[20] J. Wang, K. Atallah, R. Chin, W. M. Arshad, and H. Lendenmann, “Rotor eddy-current loss in permanent-magnet brushless AC machines,”IEEE Transactions on Magnetics, vol. 46, no. 7, pp. 2701–2707, 2010.

[21] V. Reinbold, E. Vinot, L. Garbuio and L. Gerbaud, "Magnetic Circuit Model: A Quick and Accurate Sizing Model for Electrical Machine Optimization in Hybrid Vehicles," *2014 IEEE Vehicle Power and Propulsion Conference (VPPC)*, Coimbra, 2014, pp. 1-5.